Eur. J. Mineral.
2006, **18**, 21–33

Serpentinites in an Alpine convergent setting: Effects of metamorphic grade and deformation on microstructures

ANNE-LINE AUZENDE[a, b]*, STÉPHANE GUILLOT[c], BERTRAND DEVOUARD[d] and ALAIN BARONNET[a]

[a]Centre de Recherche en Matière Condensée et Nanosciences, CNRS, campus de Luminy, F-13288 Marseille cedex 09, France
[b]present address: Institut de Minéralogie et de Physique des Milieux Condensés, CNRS UPMC IPGP, case 115, 4 place Jussieu, F-75252 Paris cedex 05, France
*Corresponding author, e-mail: auzende@impmc.jussieu.fr
[c]Laboratoire de Sciences de la Terre, CNRS UCB ENS-Lyon, bâtiment Géode, 2 rue Dubois, F-69622 Villeurbanne cedex, France
[d]Laboratoire "Magmas et volcans", CNRS UBP OPGC, 5 rue Kessler, F-63038 Clermont-Ferrand cedex, France

Abstract: Alpine antigorite serpentinites associated with eclogites were investigated to determine if they can be used as indicators of the tectono-metamorphic conditions during subduction and exhumation processes. The detailed petrology of serpentinites sampled in the Monviso massif (Western Alps, Italy) was combined with a transmission electron microscopy study. Alpine serpentinites display a degree of serpentinization close to 100%. Antigorite is the main mineral present, forming non-pseudomorphic textures in the various studied samples and exhibiting a homogeneous chemical composition with limited cationic substitutions. Considering its oceanic origin, the Alpine serpentinite in the Monviso massif formed a lizardite + chrysotile assemblage that recrystallized under greenschist-facies conditions into poorly ordered antigorite, with a modulation wavelength showing significant variations at the crystal scale. Under blueschist-facies conditions, the modulation wavelength of antigorite becomes regular. Thus, periodic antigorites can be related to high-grade conditions, while poorly ordered antigorites characterize lower metamorphic grade. In the present study, we failed to observe any elimination of structural defects with increasing metamorphic grade. While around 50% of the antigorite crystals are highly ordered, it seems that this ordering is at least partly obliterated by retrogressive deformation. Antigorite displays strong evidence of deformation-sensitivity, and the observed microstructures can be directly related to the mechanical behaviour of serpentinites in subduction zones. We investigated the deformation-induced microstructures in serpentinites collected in the Erro-Tobbio eclogitic unit (Ligurian Alps, Italy), which appear to preserve prograde and retrograde structures formed during subduction. According to the microstructural evidence, shearing is accommodated by brittle and/or ductile deformation mechanisms. Collected samples were fractured at different scales (cm to nm) and have a well-developed schistosity characterized by a strong crystallographic fabric. With increasing metamorphic grade, the brittle behaviour gives way to pressure-solution, which persists up to eclogite-facies conditions. The common obliteration of high-grade microstructures in antigorite, as observed in the Monviso serpentinites, results from continuous recrystallization of this mineral during retrogressive deformation.

Key-words: serpentinite, antigorite, HP-LT metamorphism, microstructures, deformation, pressure solution.

1. Introduction

Serpentinites result from the hydration of the oceanic upper mantle during ocean floor spreading (*e.g.* Mevel, 2003 for review) or are produced by hydration of the mantle wedge above the subducting lithosphere (Fyfe & McBirney, 1975; Guillot *et al.*, 2001; Hyndman & Peacock, 2003). They are composed of serpentine minerals, which are 1:1 type hydrous phyllosilicates of ideal formula $Mg_3Si_2O_5(OH)_4$. The low-grade phases lizardite and chrysotile result from seawater interactions during oceanic hydrothermal alteration (Evans *et al.*, 1976; Berman, 1988; O'Hanley, 1996; Mevel, 2003; Evans, 2004), while antigorite rapidly becomes stable along a cold subduction-related geotherm (Fig. 1). The antigorite structure results from a structural modulation of the serpentine layers along the **a** direction (Fig. 2a). The modulation consists of a polarity reversal of the tetrahedral sheets, with an alternation of 6-reversals (6-membered tetrahedral rings) and 8-reversals (8- and 4-membered tetrahedral rings) every half wavelength (Zussman, 1954; Zussman *et al.*, 1957; Kunze, 1956, 1958, 1961; Yada, 1979; Spinnler, 1985; Dodony *et al.*, 2002; Grobety, 2003; Capitani & Mellini, 2004). The unit cell is described by a long *A* parameter, which corresponds to the modulation wavelength along **a**,

0935-1221/06/0018-0021 $ 5.85
DOI: 10.1127/0935-1221/2006/0018-0021

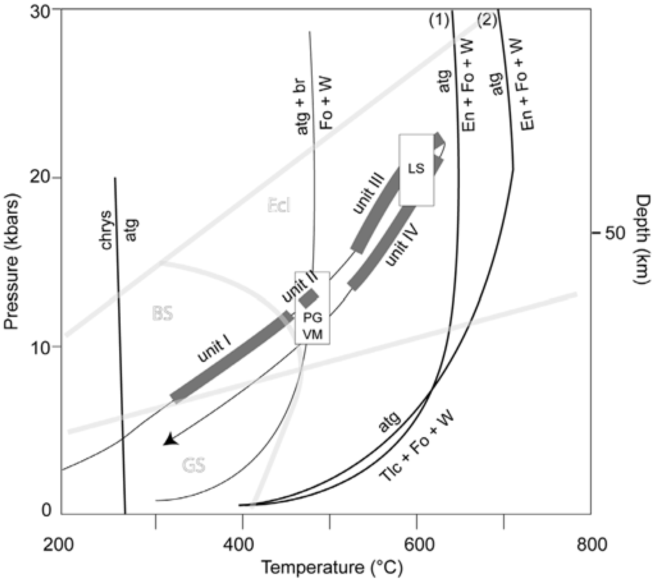

Fig. 1. Phase diagram of serpentine minerals showing P-T conditions affecting the serpentinites during their metamorphism. The boxes correspond to the estimated P-T fields of serpentinites from the Monviso massif (after Schwartz *et al.*, 2001). The thick grey lines along the Alpine P-T path correspond to metamorphic conditions undergone by the highly sheared Erro-Tobbio serpentinites (after Hermann *et al.*, 2000). Two antigorite breakdown curves are reported, derived from recent experimental studies: (1) Wunder *et al.* (2001) and (2) Ulmer & Trommsdorff (1995). The stability field of eclogite (Ecl), blueschist (BS) and greenschist (GS) facies are also indicated.
(LS = Lago Superiore, PG = Passo Gallarino and VM = Viso Mozzo; atg: antigorite, chrys: chrysotile, Fo: forsterite, En: enstatite, Tlc: talc, W: water)

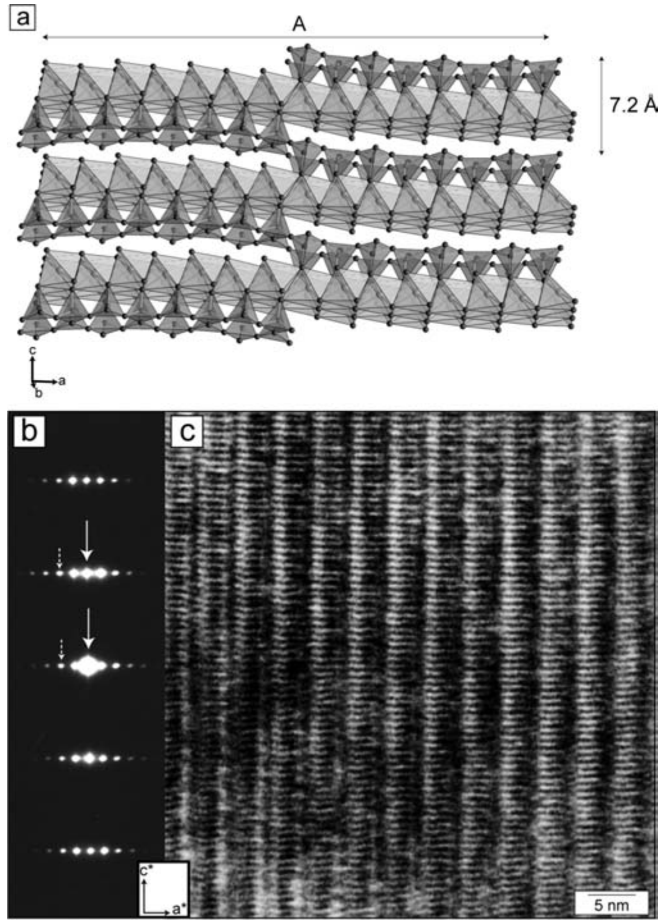

Fig. 2. a) Crystal structure of antigorite close to the a-c projection (from Uehara, 1998). b) Central zone of a Selected Area Electron Diffraction pattern of antigorite. The solid white arrow indicates a main diffraction spot and the dashed white arrow a ?surstructure satellite diffraction spot. c) High-resolution Transmission Electron Microscopy image of antigorite. Contrasts emphasize the layer thickness along a and the modulation along c.

and a layer thickness of 7.2 Å characteristic of serpentine minerals. The *A* parameter is commonly expressed by the *m*-value, representing the number of tetrahedra in one modulation. For the purposes of the present study, we mainly use this notation. Antigorite displays highly variable microstructures, such as modulations in wavelength and layer stacking. These commonly observed structural modifications are described in further detail in this paper. To some extent, Transmission Electron Microscopy (TEM) is a convenient tool for investigating and characterizing antigorite variability at such a scale. A Selected Area Electron Diffraction (SAED) pattern consists of the main diffraction spots from the lizardite subcell (white arrows, Fig. 2b), which are surrounded by satellite diffraction spots from the modulated structure of antigorite (dashed arrows, Fig. 2b). The contrasts seen on TEM images underline the layer thickness along **c** and the modulation along **a** (Fig. 2c). Only the 8-reversals produce a significant TEM contrast with the surrounding structure along **a**.

Serpentinites are observed in various active tectonic settings (*e.g.*, O'Hanley, 1996). Recently, they have been invoked as playing an important role in subduction-related processes such as exhumation of high pressure – low temperature (HP-LT) rocks (Blake *et al.*, 1995; Hermann *et al.*, 2000; Schwartz *et al.*, 2001; Guillot *et al.*, 2000, 2001), recycling water in the mantle (Scambelluri *et al.*, 1995; Ulmer & Trommsdorff, 1995; Scambelluri *et al.*, 2001) or in magma genesis leading to arc volcanism (Scambelluri *et al.*, 1995; Hattori & Guillot, 2003). These different studies give rise to some questions on the behaviour of serpentinites under subduction conditions.

Previous studies have proposed that antigorite microstructures may be used to indicate the metamorphic grade (Mellini *et al.*, 1987; Wunder *et al.*, 2001; Auzende *et al.*, 2002). Our paper presents a study of serpentinites collected in a well-constrained paleo-subduction zone (Western and Ligurian Alps), with the aim of investigating the metamorphic record. The second part of this study discusses the behaviour of serpentinites subjected to deformation, based on microstructural observations. Indeed, serpentinites are commonly highly sheared in subduction zones and the processes involved in accommodating the deformation are not clearly understood. However, the development of serpentinite deformation is a crucial issue, particularly for understanding the role of such rocks in the preservation and exhumation of HP-LT eclogites.

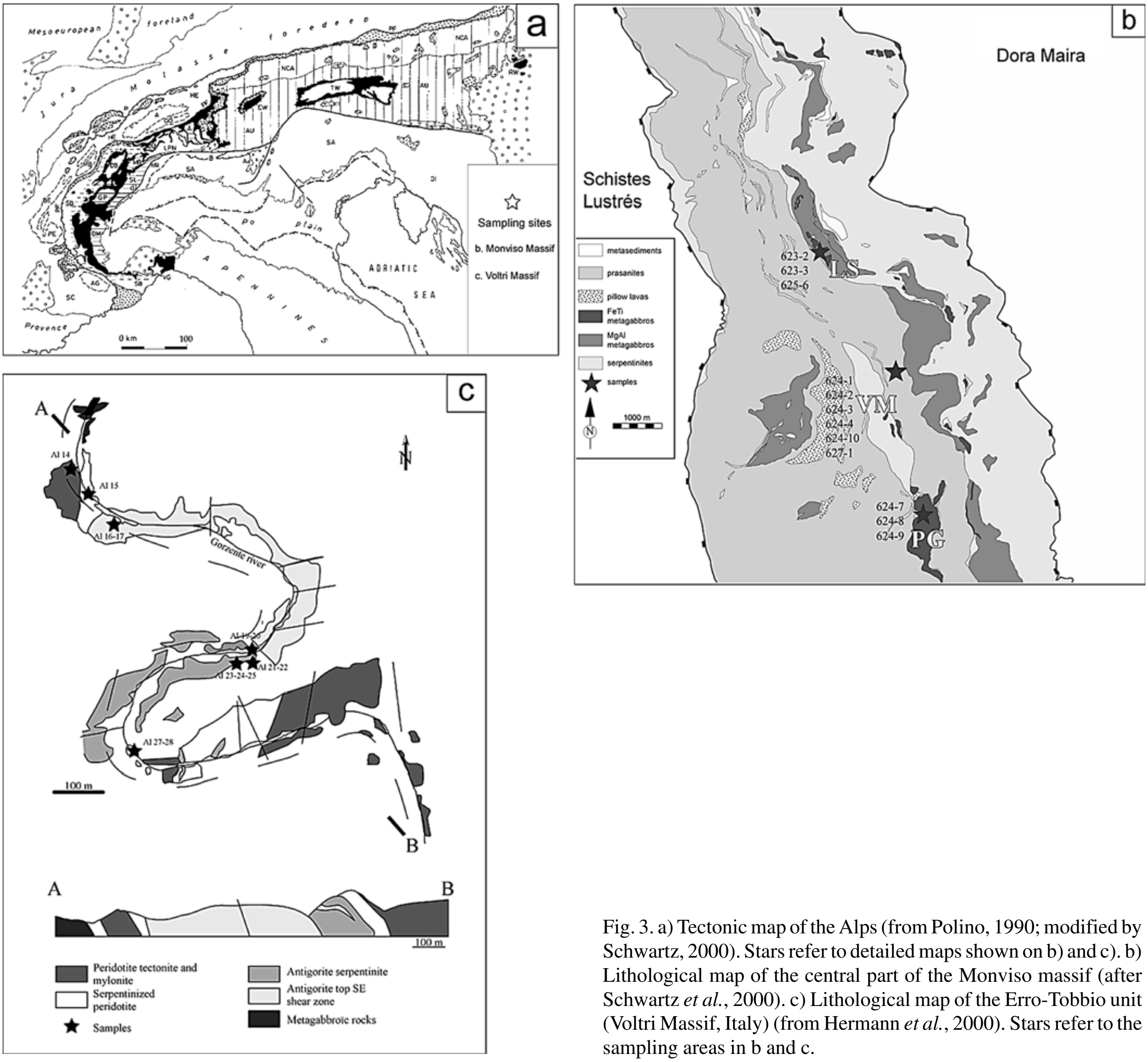

Fig. 3. a) Tectonic map of the Alps (from Polino, 1990; modified by Schwartz, 2000). Stars refer to detailed maps shown on b) and c). b) Lithological map of the central part of the Monviso massif (after Schwartz *et al.*, 2000). c) Lithological map of the Erro-Tobbio unit (Voltri Massif, Italy) (from Hermann *et al.*, 2000). Stars refer to the sampling areas in b and c.

2. Sampling and analytical conditions

2.1. Geological setting and selected serpentinite samples

To investigate the evolution of serpentine microstructures as a function of metamorphic grade, we require a well-constrained sampling zone where serpentinites are associated with metamorphic rocks that have undergone various pressure and temperature conditions along a cold geotherm. The western Alps represent a geologically well-known and serpentinite-rich terrain offering a very favourable setting for such a study (Fig. 3). The Monviso eclogitic massif (internal Piemontese zone) consists of a tectonic mélange of oceanic lithospheric fragments that have undergone Alpine subduction. Serpentinites represent about 40 % of this massif (*e.g.*, Lagabrielle, 1987; Blake *et al.*,1995; Schwartz *et al.*, 2001). The samples were collected in three units: Lago Superiore (LS), Passo Gallarino (PG) and Viso Mozzo (VM). These units correspond to a mixing of basic and ultrabasic rocks sampled at different depths, from 30 to 80 km, along the same subduction plane (Messiga *et al.*, 1999; Schwartz *et al.*, 2001). The rocks from the Lago Superiore unit have recorded high-grade eclogite-facies conditions ($P = 19 \pm 2$ kbar, $T = 580 \pm 40$ up to $P > 24$ kbar, $T = 620 \pm 50$°C; Schwartz *et al.*, 2001 and Messiga *et al.*, 1999, respectively) while the two other units have undergone conditions at the transition between the blueschist and eclogite facies (12–13 kbar, $T = 450 \pm 40$°C). Since the serpentinites are intimately associated with eclogites in the field from the cm to the cartographic scale, we assume they have shared a similar metamorphic evolution (*e.g.*, Schwartz *et al.*, 2001). The metamorphic conditions are illustrated in Fig. 1. We studied serpentinites collected in lenses embedded in a protecting matrix, since these lenses are more likely to preserve the structures acquired during the metamorphic peak. However, in the Monviso massif, the embedding matrix consists mainly of highly sheared serpentinites that are harder compared with the soft metasediments surrounding the serpentinites lenses in Cuba (Auzende *et al.*, 2002).

To investigate the deformation-induced microstructures of antigorites sheared at high grade, we selected serpentinite samples from the Erro-Tobbio (ET) unit (Fig. 3) in the Voltri massif (Ligurian Alps, Italy). This massif, which is located at the transition between the Alps and the Apennines, belongs to the internal Penninic domain and consists of three units corresponding to remnants of the Liguro-Piemontese oceanic lithosphere (Chiesa *et al.*, 1975; Piccardo, 1984; Piccardo *et al.*, 1988; Messiga & Scambelluri, 1991). The Erro-Tobbio unit is the uppermost unit in the stacking sequence of this tectonic domain. This unit underwent a similar tectonic history compared with the Monviso massif: i) exhumation of subcontinental mantle during Alpine rifting, ii) emplacement onto Tethyan ocean floor, iii) subduction during convergence between Africa and Europe, and iv) exhumation and emplacement at its present position. The serpentinites and associated shear zones have preserved and recorded these successive Alpine events, and the successive ductile and brittle deformation structures are correlated with the successive P-T conditions (Hermann *et al.*, 2000) as shown on Fig. 1.

2.2. High-resolution transmission electron microscopy

TEM imaging and electron diffraction data were acquired with a JEOL 2000FX high-resolution transmission electron microscope at the CRMCN-CNRS facility (Marseille, France). The operating conditions were: 200 kV accelerating voltage, a point-to-point resolution of 2.8 Å, using a side entry, double-tilt (± 30°) specimen holder. The TEM specimens were extracted from petrographic thin sections glued with Crystal Bond® epoxy resin onto a glass slide. Single-hole copper TEM slots were glued with araldite® onto selected areas of the thin sections. Specimens were removed by drilling around the Cu slots and heating the thermal resin. Prior to TEM observations, the specimens were thinned to perforation by ion-beam milling (PIPS™-Precision Ion Polishing System- GATAN® 691) and then carbon coated.

Antigorite along the [010] direction can be easily recognised on TEM images and SAED patterns owing to its modulated structure (Fig. 2). Most of the crystals were oriented along [010]. TEM observations were performed on selected domains, petrologically characterized by a homogeneous texture and the absence of visible retrogressive veins.

3. Results

3.1. Monviso serpentinites

Prior to the TEM study, we characterized the samples petrologically. Observations at the mm scale allowed us to select representative unretrogressed areas for TEM studies. The serpentinites collected in the Monviso unit are homogeneous, with a degree of serpentinization close to 100 %. A few samples also contain relict diopside grains, which are highly serpentinized and deformed. Serpentine minerals occur as interpenetrative blades in non pseudomorphic textures. Ghosts of early pseudomorphic structures can be observed with relict magnetites that still outline the early mesh boundaries. Former serpentinized pyroxenes (bastites) correspond to magnetite-free areas (Fig. 4a). Figure 4 also shows high-grade recrystallization of the serpentine into interpenetrative blades in the cores of meshes and in bastites. However, we can differentiate these textures from the classical pseudomorphic textures described by Wicks & O'Hanley (1988). Textural evidence combined with a micro-Raman spectroscopic study (ENS-Lyon) show that antigorite is

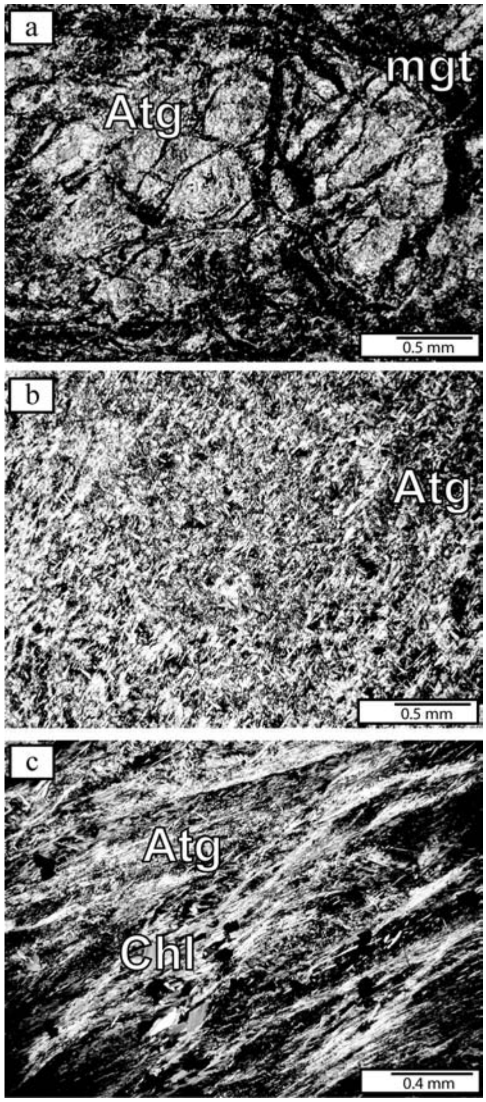

Fig. 4. Microphotographs under cross-polarized light of thin sections of serpentinites from Monviso. a) Interpenetrative antigorite texture with preserved pseudomorphic mesh boundaries picked out by magnetite (serpentinite 624–2 : Viso Mozzo). b) Typical antigorite interpenetrative texture within a former bastite (serpentinite 623–3: Lago Superiore). c) Sheared serpentinite with antigorite and chlorite (Chl) defining the cleavage. Some postkinematic chlorite crystals cut the foliation (serpentinite 625–6 : Lago Superiore).

Table 1. Representative chemical analyses of antigorites from Monviso.

	LS 623–2	LS 623–3	LS 625–6	PG 624–9	PG 624–8	PG 624–7	VM 624–4	VM 624–10	VM 627–1
SiO_2	42.23	43.43	41.77	43.53	42.88	41.50	42.67	42.04	41.60
Al_2O_3	2.14	1.35	2.87	1.37	1.73	2.60	2.24	2.07	1.97
FeO	2.92	1.92	6.50	3.18	3.57	3.57	3.21	3.24	2.46
MgO	39.10	39.84	35.78	38.46	38.36	37.60	38.50	38.76	39.99
Total	86.40	86.54	86.92	86.55	86.54	85.27	86.62	86.11	86.01

the main variety in these samples, while classical meshes are usually considered as being composed of lizardite (Wicks & O'Hanley, 1988). An exception occurs in the Lago Superiore serpentinite sample 625–6, which exhibits an intimate association between antigorite and chlorite (Fig. 4c). Most of the samples contain late veins filled by minerals such as chlorite or fibrous chrysotile. Electron microprobe analyses (Cameca SX100 – Clermont-Ferrand) fail to show any clear variation of antigorite composition. Antigorites are magnesium-rich (Table 1 and Fig. 5), with substitution of aluminium and iron remaining below 10 wt% (oxide weight). The higher amount of Al_2O_3 and FeO (> 10 wt%) in sample 625–6 is the result of the intimate mixing of antigorite and chlorite.

At the TEM scale, the antigorite microstructures were investigated by electron imaging coupled with SAED. The results show that, while the samples are homogeneous at the micron scale (as regards texture and chemistry), antigorite crystals display a high variability. However, we note one constant feature in all the SAED patterns: the presence of sharp modulation diffraction spots without streaking in the **a*** direction (Fig. 6). This emphasizes the regularity of intracrystalline polysomatic structures in the Monviso samples, *i.e.*, the *A* dimension (modulation wavelength) is constant at the crystal scale. This regularity is also clearly noticeable on TEM images, showing highly ordered structures along **a** (Fig. 6). Nevertheless, while the modulation length is constant in each crystal, this dimension significantly varies from one antigorite grain to another within the same TEM sample. The *m*-values, which express the modulation wavelength, range from 13 (Mellini & Zussman, 1986) to 50 (Chapman & Zussman, 1959; Grobety, 2003), while most antigorites display $m = 13$–21 (Zussman *et al.*, 1957; Kunze, 1961; Uehara & Shirozu, 1985). Polysomatic variations were quantified by measuring *m*-values from the SAED patterns of 96 antigorite crystals oriented along [010]. The results are presented on Fig. 7a. According to our data, antigorites from Monviso have *m*-values varying between 16 and 20 (41 to 52 Å), with a dominance of crystals with $m = 18$ (46 Å) and 19 (49 Å). The average *m*-values for the three units are relatively close considering their standard deviation.

We also tried to evaluate the nature and frequency of variations with respect to the basic structure of antigorite by studying the SAED patterns of the 96 antigorite crystals oriented along [010] as well as the associated electron images. In the Monviso samples, antigorite microstructures vary from highly ordered to lower periodic structures in the **c** direction (Fig. 6a-c). It is difficult to quantify the degree of order, chiefly because antigorite structures change at the crystal scale. Thus, we used SAED patterns to determine whether or not the crystals were ordered, assuming that disordered patterns exhibit diffuse streaking between subcell spots or modulation spots. Around 50 % of antigorites are highly ordered in the Lago Superiore unit, 37 % in the Passo Gallarino unit and 65 % in the Viso Mozzo unit. The other crystals display diverse amounts of structural variation. Among the different types of modification, offset is a common stacking defect characterized on the SAED pattern by satellites around the (*h00*) sublattice spots that are not lined up with the neighbouring (*h00*) group (Fig. 6b: top). This implies a difference in orientation between the sublattice and the modulated cell, which can be explained by a lateral shift of the layers along (001) planes (Spinnler, 1985; Otten, 1993). Offsets are hardly resolvable on TEM images, since they mainly involve a lateral shift of a single lizardite modulus (Fig. 6b: bottom). Almost 50 % of the investigated crystals display offsets, whatever the sample location. Another frequent type of stacking modification corresponds to polytypic variations from the common 1-layer stacking. Unusual intensity reinforcement can appear on the SAED pattern at half the distance of two successive spots along **c*** (Fig. 6c: top). Such a pattern may arise either from a 2-layer sequence or a mixing of 1- and 2-layer stacking. The electron image clears up this ambiguity (Fig. 6c: bottom). In the Monviso samples, 20 % of the crystals in the Lago Superiore unit display 2-layer stacking slabs, characterized by a layer repeat along **c** twice as long as that of the usual layer, *i.e.*, 14.6 Å, in a 1-layer sequence, 15 % in the Passo Gallarino unit and 8 % in the Viso Mozzo unit. Twinning is another type of stacking variation, which is expressed on SAED patterns by two sets of spots representing two distinct lattices slightly disoriented relatively along **b*** (Fig. 6d: left). In real space, the twinning operation can be described by combining a (001) mirror with a shift of half the modulation wavelength (Spinnler, 1985; Otten, 1993). Thus, despite being apparently out of phase due to the switch of the 8- and 6-membered reversals, the half waves remain in phase. A significant amount of these

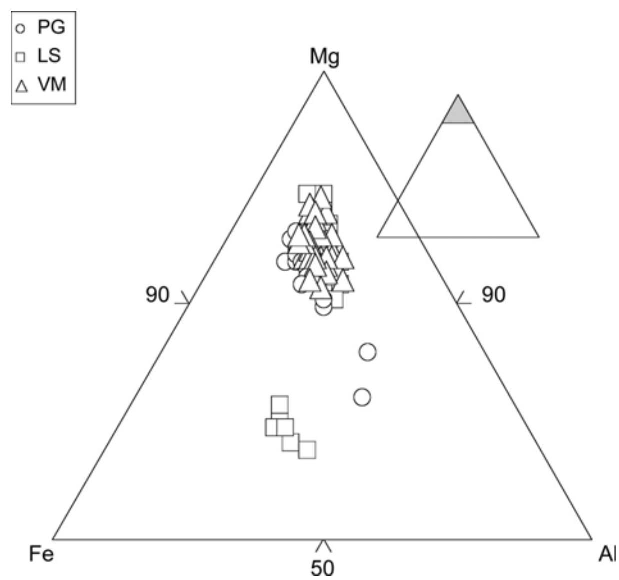

Fig. 5. Chemical composition (in atom %) of antigorites from the Monviso obtained by electron microprobe analysis (Cameca SX100 – Clermont-Ferrand).

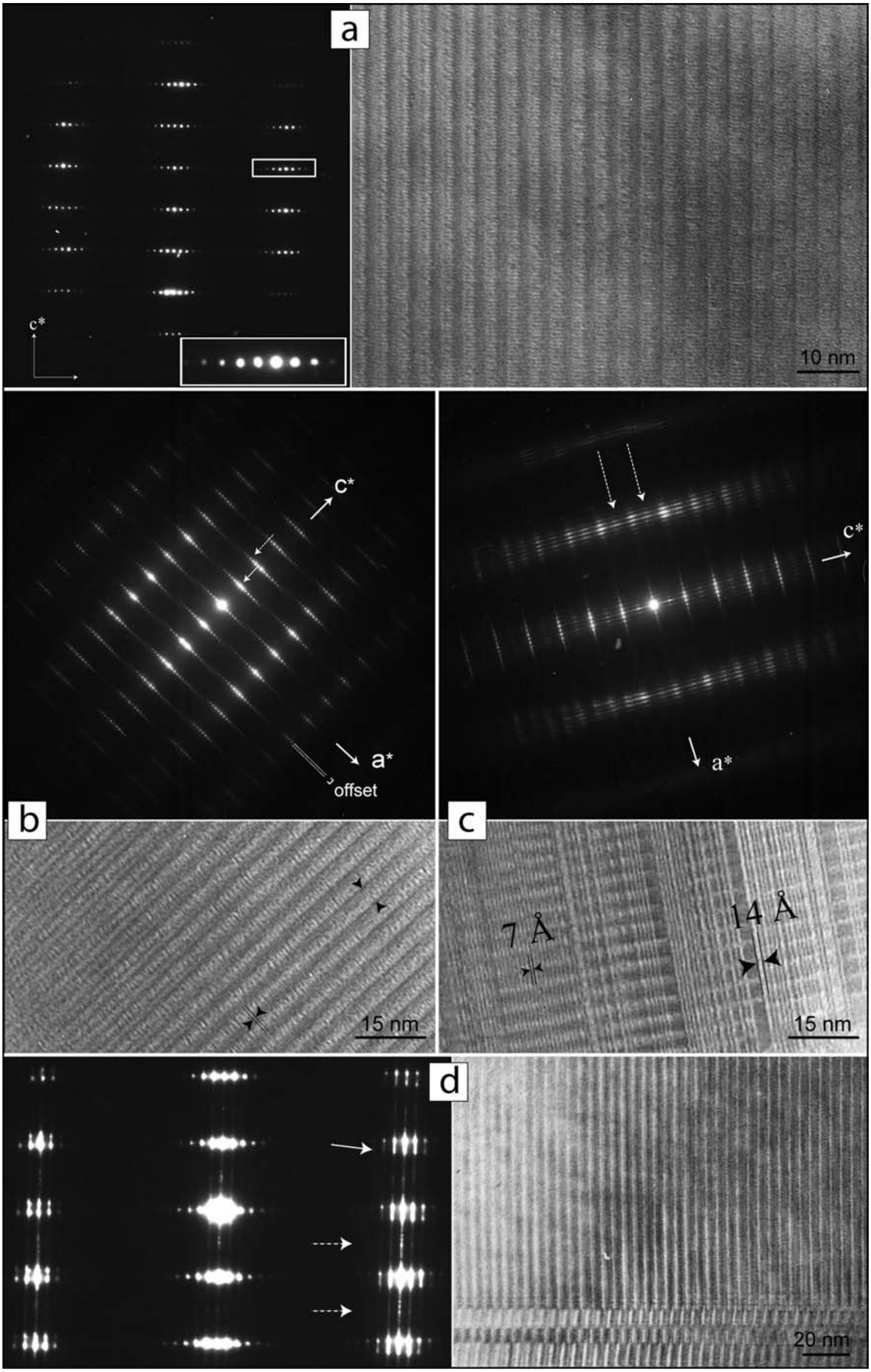
a
c*
10 nm
c*
a*
offset
b
c*
a*
c
15 nm
7 Å
14 Å
15 nm
d
20 nm

stacking faults produce a periodicity loss in the **c** direction. It also produces diffuse streaks that affect the diffraction spots along **c***. Twinning affects about 35 % of antigorites in the Lago Superiore, 53 % in the Passo Gallarino unit and 50 % in the Viso Mozzo unit.

In a general way, most of the antigorite crystals from Monviso are characterized by highly ordered portions intercalated with variably sized slabs of low-periodicity structures (Fig. 6d).

3.2. Erro-Tobbio serpentinites

The Erro Tobbio (ET) serpentinites are highly sheared. Various deformation structures are recognized, each recording a distinct deformation phase during burial (prograde units I/II and III) and exhumation (retrogressed unit IV) (Piccardo *et al.*, 1988; Scambelluri *et al.*, 1995; Hermann *et al.*, 2000). Specific P-T conditions are attributed to the successive deformation phases in the serpentinites by Hermann *et al.* (2000) (Fig. 1).

The studied samples are almost entirely serpentinized and display only some rare early diopsides in a homogeneous matrix of antigorite. The texture is clearly non pseudomorphic. The antigorite blades display a strong crystallographic fabric, defining the main schistosity but locally affected by bending related to ductile shear planes. In early serpentinites (unit I/II), the schistosity is cut by late veins filled by metamorphic olivine ± titano-clinohumite. These veins commonly affect the ET samples and can be observed at the outcrop (Fig. 8a) or at the microscopic scale (Fig. 8b). Under higher PT conditions (III), the "schistosity + cross-cutting veins" structure is replaced by a more complex system, with simultaneous development of antigorite schistosity and continuously dismembered olivine veins (Hermann *et al.*, 2000). In unit IV, cleavage and shear band structures are well-developed and shear bands are picked out by clusters of recrystallized diopside + olivine.

Similarly to the Monviso antigorites, we observed no significant intracrystalline polysomatic disorder in these samples. From the study of 58 SAED patterns of antigorite crys-

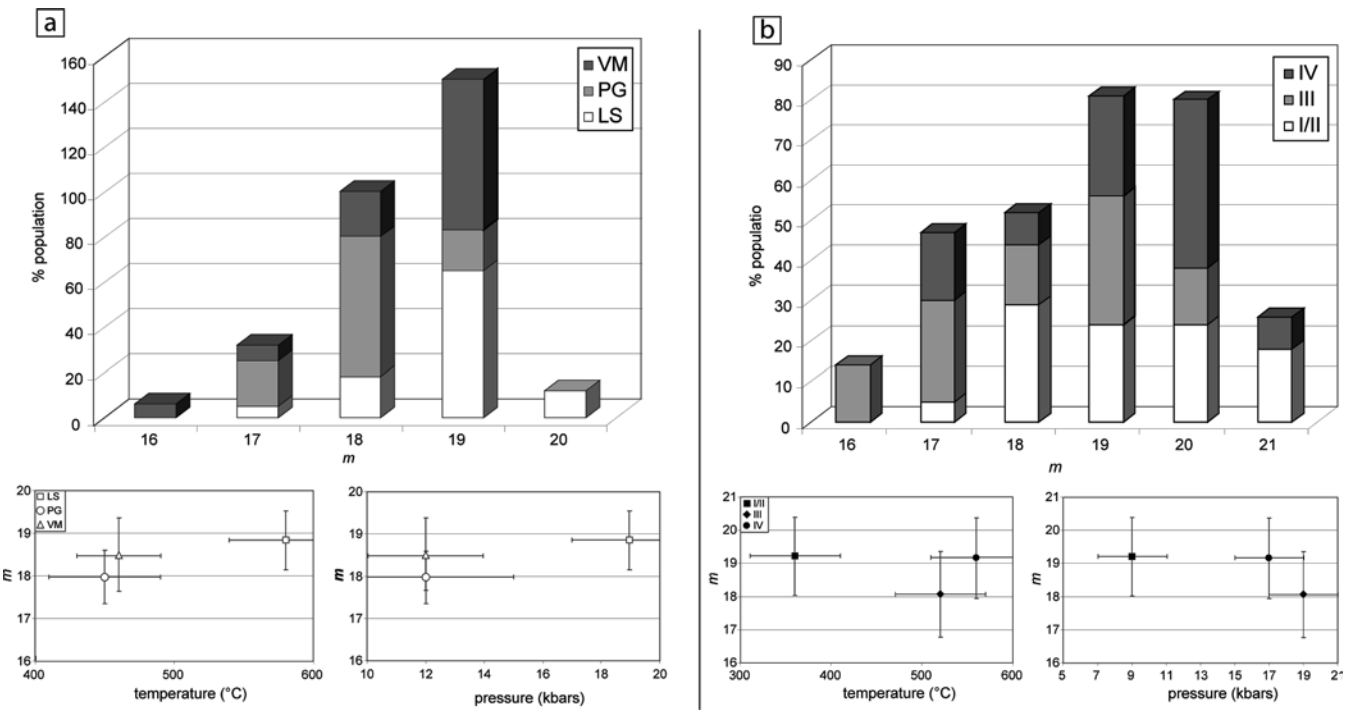

Fig. 7. Histograms representing the modulation wavelength variability (expressed by *m*-values) and associated average *m*-values as a function of pressure and temperature in a) Monviso samples (from 96 SAED patterns) and b) Erro Tobbio samples (from 58 SAED pattern). The vertical bars represent the standard derivation and the horizontal bar the uncertainties on the PT conditions. For Erro Tobbio samples, T and P uncertainties are arbitrarily defined as ± 50°C and ± 2 kbar respectively.

Fig. 6. Electron micrographs and associated SAED patterns of antigorite crystals from Monviso oriented along [010] direction. a) Highly ordered structure along a* and c*. Magnification of framed diffraction spots reveals the lack of streaking along these directions (LS, 623–3). b) Offset structure. The offset is the difference in alignment between satellites around a (*h00*) sublattice spot and around the neighbouring (*h00*) group. The lateral shift of the layers can hardly be observed on the electron image at this resolution (Passo Gallarino, 624–7). c) Stacking variations, alternating 1- and 2-layer polytypes. The dashed arrows in the SAED pattern indicate the intensity reinforcement due to the double periodicity along c*. Besides the polytypic variations, the pattern shows diffuse streaks that affect the lattice and modulation spots along c*, indicating the loss of periodicity due to planar faults/?defects. The associated micrograph show the stacking of two distinct polytypes (Passo Gallarino, 624–7). d) Streaking along c* indicates stacking disorder. White arrow shows spot rotation due to twinning and dotted white arrows indicate supplementary diffraction spot with 14.6 Å periodicity characteristic of 2-layer polytype (Monviso, Lago Superiore, 623–3).

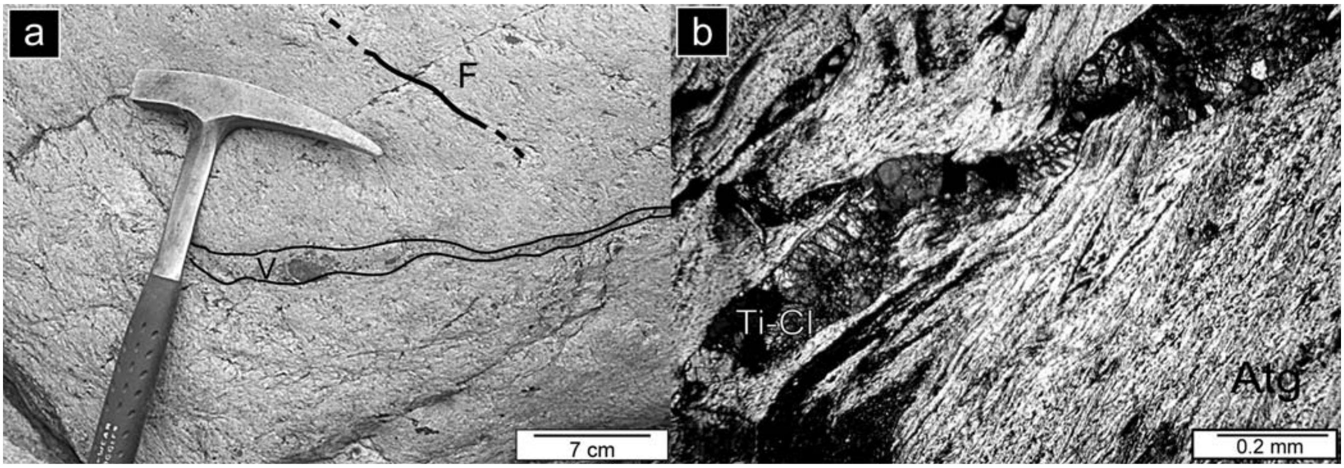

Fig. 8. a) Photograph of an "en echelon" vein (V) cutting antigorite foliation (F), filled by olivine + titano-clinohumite (Ti-Cl) (Erro Tobbio-Al22). b) Microphotograph of a foliated serpentinite under crossed Nicols. Olivine-TiCl vein crosscut the ductile structures (Erro Tobbio-Al28).

tals oriented along [010], the distribution of *m*-values for ET samples appears somewhat broader compared to Monviso (Fig. 7b). This reflects a greater variation of the modulation wavelength, with *m*-values ranging from 16 to 21 (41 to 54 Å). When plotted against pressure and temperature, the average *m*-values do not show any clear trend. Locally, ET antigorite crystals are highly disordered with numerous stakking faults (Fig. 9a). Twinning and offset structures are the most common defects in these antigorites, affecting around 50 % of the crystals. The 2-layer polytypes also occur as intergrowth slabs in mainly 1-layer crystals, as in Monviso, and appear in up to 46 % of the investigated crystals in unit III.

As previously mentioned, deformation structures can be recognized at various scales from optical microscopy and field observations. Figure 9a presents a high-resolution TEM image of antigorite from a sheared ET sample (unit II). The two blocks of antigorite are affected by numerous stakking faults. The grain boundary between the two blocks is irregular, occurring as an interpenetrative contact similar to a grain suture between deformed crystals of other minerals (*e.g.*, Blenkisop, 2000 for review). Furthermore, several stacking faults can be traced on both sides of the boundary, both far away as well as close to the contact. The slight disorientation of the left block has caused a loss of resolution and explains why not all the faults can be traced across. Finally, the close orientation of both blocks strongly suggests that an initial antigorite grain was broken into these two blocks by microfracturing. The shift of the common defects within the two blocks suggests that the two parts have moved relative to one another. The fracture picks out brittle deformation that is also observed at a larger scale (Fig. 8). In the area outlined by the square in Fig. 9a, brittle deformation has now been replaced by ductile deformation. We observe rotations of modulation along **a** that are caused by ductile deformation of the edges of the blocks. In the investigated crystal, these rotations mainly occur about the [010] direction. The movements of these blocks have created empty spaces that have been infilled by recrystallization of new antigorite. On Fig. 9b, antigorite recrystallization is more developed. The variations in contrast are due to the relatively slight disorientation of the two parts, which picks out a grain boundary indicated by the dashed line. As in the previous image, the contact resembles an interpenetrative suture. The lack of significant stacking disorder and the disorientation of the bottom block means we are unable to observe any relative shifts of the blocks. Significant recrystallization of antigorite is only observed in the high-grade Erro Tobbio serpentinites. Ductile deformation mechanisms are suspected in these serpentinites, since they display well-developed cleavage and strong crystallographic orientation.

4. Discussion

4.1. Do antigorite microstructures yield a record of metamorphic conditions?

We can evaluate the metamorphic conditions recorded by rocks in several ways. One of the most effective methods is to study the mineral reactions that reflect the metamorphic evolution of the rocks. Geochemistry can also be used, since the composition of mineral solid-solutions can give reliable information on the preserved P and/or T conditions. However, while there is no simple tool to estimate the P-T conditions in serpentinites, some insights can now be provided by the structural variations. The Monviso Serpentinites have undergone Alpine metamorphism. During burial and exhumation, they underwent variations in pressure and temperature up to eclogite-facies conditions. When embedded in a suitable matrix, the samples were protected from retrogressive alteration during exhumation, thus preserving a possible record of the metamorphic climax, as observed within the serpentinites from central Cuba (Auzende *et al.*, 2002).

Most Alpine serpentinites have an oceanic origin, and this is notably the case for Monviso (Phillipot *et al.*, 1993, 1998; Lagabrielle & Lemoine, 1997). The petrology of oceanic serpentinites is clearly established, and usually consists of an assemblage of lizardite and chrysotile (*e.g.*, Wicks & O'Hanley, 1988; Mevel, 2003 for a review). During the first

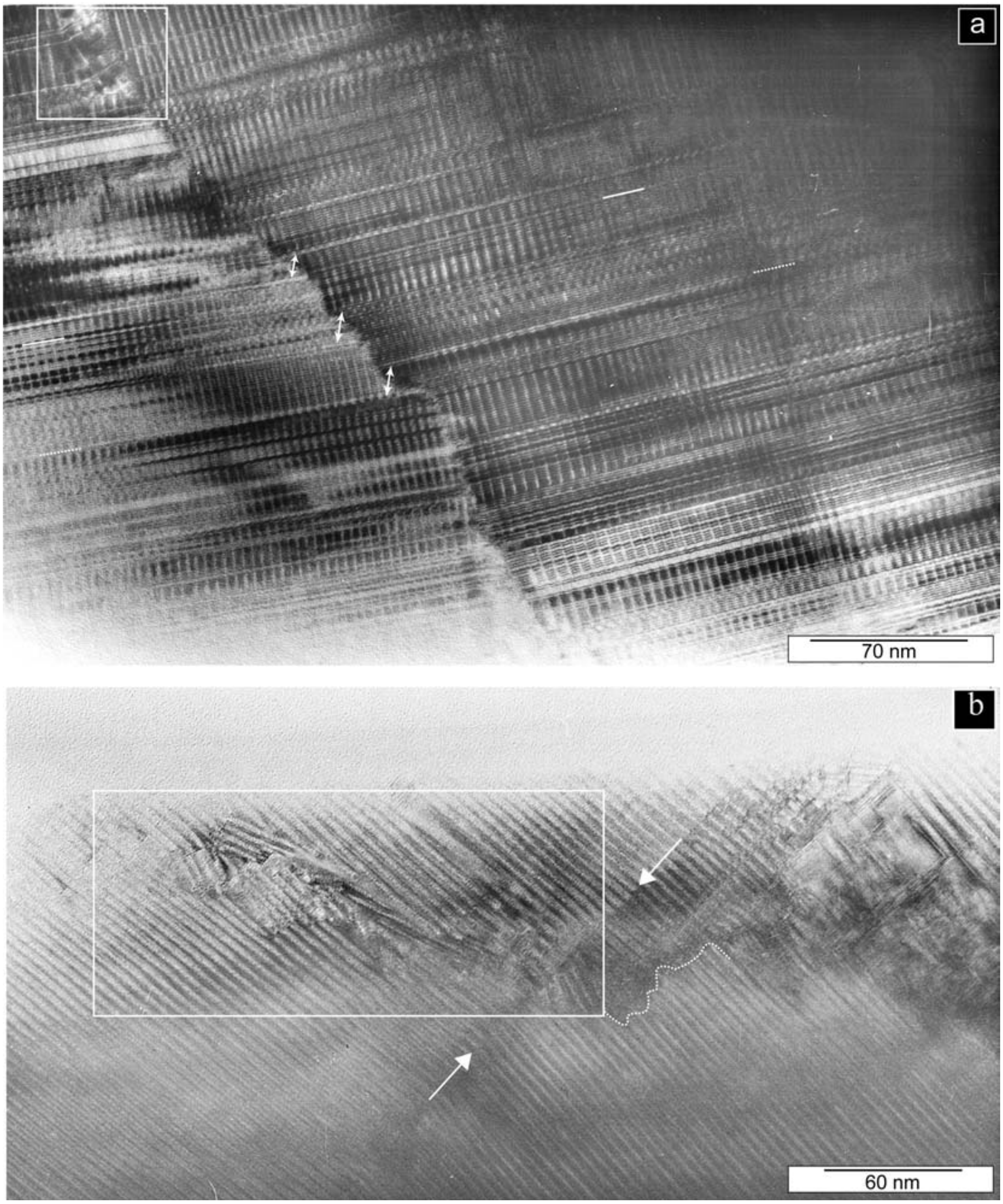

Fig. 9. a) Electron microphotograph of an antigorite monocrystal affected by a microfault. Defects in both parts can be correlated across the suture zone, as indicated by the white arrows. The zone outlined by the square displays ductile modulation rotation and antigorite recrystallization (Erro Tobbio-Al21).
b) Electron micrograph of a grain boundary with intense antigorite recrystallization (Erro Tobbio-Al21).

stages of burial under greenschist-facies conditions, the subducting oceanic serpentinite transforms into a metamorphic assemblage dominated by antigorite that persists up to high pressure (> 6 GPa) (Ulmer & Trommsdorff, 1995; Wunder & Schreyer, 1997; Wunder *et al.*, 2001). This mineralogical reaction is considered as an early record of increasing metamorphic grade within serpentinites. This is effectively the case for the Monviso samples, which are dominated by antigorites. This metamorphic reaction is accompanied by textural modifications: pseudomorphic lizardite textures are progressively replaced by interpenetrative, non-pseudomorphic antigorite textures. Therefore, this early stage in the prograde metamorphic record can be observed at the thin-section scale.

The study of antigorite microstructures from Monviso by TEM reveals a systematic intracrystalline polysomatic order. The periodicity of the modulation wavelength is preserved whatever the frequency of other structural faults. This is in agreement with previous results acquired on Cuban serpentinites (Auzende *et al.*, 2002). On the other hand, this is in contrast with the high degree of intracrystalline polysomatic disorder commonly observed in antigorites that have not undergone high-pressure conditions. Indeed, “accordion-type” structures have been observed in the Val Malenco antigorites (Mellini *et al.*, 1987) and in antigorites in veins (Viti & Mellini, 1996). In matrix antigorites from the Malenco ophiolitic nappe, Mellini *et al.* (1987) observed a polysomatic disorder in the antigorite crystallites of low-grade serpentinites that can persist up into greenschist-facies metamorphic conditions. This polysomatic disorder is enhanced in antigorite crystals thermally recrystallized due to contact metamorphism, while a higher pressure sample (MG159, upper greenschist-facies conditions) is well-ordered. According to the results of Mellini *et al.* (1987) and our study, ordering of the modulation may be achieved under blueschists-facies conditions. Therefore, the elimination of intracrystalline polysomatic disorder can be correlated with increasing metamorphic grade in a subduction context.

Mellini *et al.* (1987) and Wunder *et al.* (2001) proposed that the recorded metamorphic grade is a function of the modulation wavelength of antigorites. Mellini *et al.* (1987) investigated natural antigorites recrystallized at low pressure and high temperature during the contact metamorphism associated with the intrusion of the Alpine Bregaglia phonolitic massif. Wunder *et al.* (2001) carried out their study on antigorites synthesized at various PT conditions in the pure MSH system. According to these studies, the *m*-value describing the modulation wavelength decreases with temperature. This temperature effect is not confirmed in our study within the investigated range. Wunder *et al.* (2001) showed a T-dependence of *m*, with values varying from 18 at the lowest temperature to 14 at the temperature of antigorite breakdown. According to these authors, antigorites from Monviso should display *m*-values around 14 and 15 instead of the values we obtained around 18 or 19. The discrepancy between our data and the experimental results of Wunder *et al.* (2001) may tentatively be explained by the chemical differences between the antigorites. Indeed, the Monviso antigorites contain significant amounts of iron and aluminium (3–4 wt% FeO_t and 2–3 wt% Al_2O_3) (see Fig. 5 and Table 1) while the synthetic antigorites of Wunder *et al.* (2001) are purely magnesian. However, even though substitutions may change the wavelength compared to purely magnesian antigorites, this is not yet clearly established, so chemical variations cannot entirely explain this discrepancy. Indeed, as the Monviso antigorites exhibit homogeneous chemistry, substitutions would only shift the *m*-values ranges. Furthermore, Mellini *et al.* (1987) also studied natural substituted samples. The main difference with our study is that Mellini *et al.'s* (1987) samples underwent increasing temperature conditions but only a limited rise in pressure. We assume that pressure may also be an important factor that might change the value of *m* set by the temperature conditions. Finally, it is important to note that the processes of antigorite growth are unknown. Thus, parameters such as the surrounding oxidation state or the rock-water ratio may play an important role in explaining the wavelength of the modulation. We propose here that *m*-values cannot be used in natural high-grade antigorites as a T-indicator or P-indicator. This is also consistent with results obtained on the Cuban serpentinites (Auzende *et al.*, 2002).

The ordering of microstructures with increasing metamorphic grade has already been observed in carbonaceous materials (Beyssac *et al.*, 2002), and as a function of pressure in phyllosilicates such as the chlorite cookeite (Jullien *et al.*, 1996) and talc (Jullien, 1995). Such an effect was suggested for antigorite microstructures (Auzende *et al.*, 2002). In the Monviso samples, while half of the crystals are highly ordered, the remainder display considerable stacking disorder. We observed perfectly ordered high-grade antigorites, while low-grade antigorites are mainly disordered, which suggests that increasing metamorphic grade tends to order the structure. However, the lack of statistically-significant evidence for the evolution of ordering within the studied range of P-T conditions prevents us from using antigorite as a reliable thermobarometer in subduction settings. The main difference between Cuban and Alpine serpentinites may arise from the quality of preservation. While Cuban serpentinites from the Escambray massif are embedded in a matrix of weak metasediments, the Monviso samples are embedded in a matrix of sheared serpentinites. Thus, the rheological boundary observed in Cuba may not be as efficient in the Alpine example. Indeed, the viscosity of metasediments is at least an order of magnitude lower than that of serpentinites (*e.g.*, Schwartz *et al.*, 2001). This could explain the occurrence of retrogressed veins at the mm scale as well as the possible non-preservation of a modulation wavelength characteristic of high metamorphic grade.

4.2. Do antigorite microstructures provide evidence of deformation processes?

Multi-scale observations of highly-sheared serpentinites that experienced varying P-T conditions along a cold geotherm have different coexisting deformation structures in most samples.

The veins expressing brittle deformation are filled with metamorphic olivine ± titano-clinohumite, which are the dehydration products of serpentines (Hermann *et al.*, 2000). This demonstrates that the Erro Tobbio serpentinites have experienced partial breakdown of antigorite and is consistent with several studies showing that serpentinites become brittle when they reach dehydration conditions (Raleigh & Patterson, 1965; Escartin *et al.*, 1997; Neufeld *et al.*, 2003). This brittle behaviour is also seen at the TEM scale, where we observe antigorite crystals affected by microfractures (Fig. 9).

Brittle behaviour is not the only way for serpentinites to accommodate deformation. Raleigh & Paterson (1965) showed that below 600°C, and with increasing pressure, serpentinites composed of antigorite and chrysotile go from a brittle to a ductile behaviour. However, because the pressure range given by these authors (*op.cit.*) does not exceed 5 kbar, these assemblages can hardly be compared to our samples. At the field and thin-section scale, ductile deformation is indicated by antigorite schistosity marked by a strong crystallographic fabric. Various mechanisms can produce schistosity, but phyllosilicates such as micas or chlorites are known to accommodate deformation mainly by gliding on (001) planes (Bons, 1988 for chlorite; Etheridge & Schreyers, 1973, Kronenberg, 1990, Christoffersen & Kronenberg, 1993 for biotite; Mares & Kronenberg, 1993 for muscovite). Antigorite, as the other phyllosilicates, displays a lower density of iono-covalent bonds along [001] with respect to directions in the (a,b) plane (Kunze, 1961; Capitani & Mellini, 2004). However, the successive layers of antigorite are linked at every half wavelength by strong Si-O-Si bonds along **c** (Fig. 2). This makes basal slips more difficult compared with the other phyllosilicates. In this study of Erro Tobbio antigorites, we show that half of the investigated crystal display mildly ordered structures, with offsets or twinning. Most of the stacking faults are characterized, at least partly, by a gliding component along **a** (*e.g.*, Spinnler, 1985; Otten, 1993). A twin is also a structure that can be related to deformation (*e.g.*, Blenkishop, 2000). In antigorite, it is not clear whether twins represent a structure related to growth or deformation. The previous crystallographic explanation of twinning implies that it is unlikely to result from deformation. Moreover, the Monviso antigorites display a similar proportion of twins compared to the Val Malenco antigorites, which recrystallized under static conditions (Mellini *et al.*, 1987). Even if these defects are shearing-related, which remains to be demonstrated, their role in deformation accommodation is not evident. The complex operation that produces twinning implies severe crystallographic constraints, such as the coincidence of reversals. This suggests that twinning might be a less efficient mechanism compared with common basal slips, where adjustment of the successive layers is easy. In contrast, offsets would be more likely explained by deformation. However, we were unable to find any significant increase of the amount of these defects in the Erro Tobbio serpentinites.

Several other deformation structures are observed, especially by TEM, that might be good candidates for the accommodation of deformation. We observed ductile block rotations and antigorite recrystallizations in open interstices. The suture between the two blocks of the crystal resembles an interpenetrative contact (Fig. 9). All these features suggest the removal and reprecipitation of material by pressure solution (*e.g.*, Blenkinshop, 2000). This process is often involved in the formation of schistosity (Wood, 1974) and is considered as one of the most efficient mechanisms of deformation accommodation. Pressure solution is generally considered as a low-grade process, mainly because it requires fluids (*e.g.*, Durney, 1972; Gray, 1979; Kerrich, 1997). However, it may persist up to eclogite-facies conditions (Bell & Cuff, 1989). In our case, the required fluids may be available because of the partial dehydration of antigorites. Indeed, serpentinite dehydration produces continuous fluid release up until the complete breakdown of antigorite (Fig. 1). This implies a progressive increase of pore pressure up to a critical value which, in order to reduce the stress regime, brings the system into a brittle regime (Dobson *et al.*, 2002). Between two main events of hydraulic fracturing, *i.e.* when the pore pressure is too high, fluids are available for pressure-solution processes. Pressure solution could be the dominant deformation process in antigorite, which would also be compatible with the modelling of eclogite exhumation velocity in a serpentinite channel (Gerya & Stöckert, 2002). These authors showed that a Newtonian rheology, such as pressure solution along the subduction plane, can explain the fast exhumation rate of eclogite (1/3 of the subduction rate) better than a non-Newtonian rheology such as a power-law creep (1/6 of the subduction rate). Thus, antigorite can be considered to be synkinematic mineral that continuously recrystallizes during deformation processes. This could explain why the occurrence of antigorite is restricted to fault planes in the oceanic lithosphere. It also accounts for the difficulty of synthesizing this mineral under hydrostatic pressure conditions, while it is frequently described along the fault planes of low-grade rocks. The synkinematic crystallization also explains the non-preservation of a metamorphic microstructural record in antigorite-bearing rocks.

5. Conclusions

Serpentine microstructures can potentially preserve information on metamorphic conditions. Indeed, above the chrysotile-lizardite to antigorite transition, antigorite to some extent displays increasingly ordered structures as a function of metamorphic grade. Intracrystalline polysomatic disorder is progressively obliterated at increasing pressure and temperature. Such an increase in polysomatic order is also observed in high-grade sheared serpentinites containing antigorite. Finally, stacking disorder (along **c***) seems to decrease with increasing metamorphic grade (Auzende *et al.*, 2002). However, this last step seems to be obliterated by subsequent deformation episodes (prograde shearing as well as retrogression) and will only be observed in the best preserved rocks. This means that antigorite cannot be used as a reliable marker in subduction conditions.

The deformation processes of serpentinites during subduction are complex. Once the partial dehydration reaction is reached, antigorite could recrystallize mainly by a pressure solution mechanism, and the mineral would thus exhibit a synkinematic behaviour. The required fluids would be derived from the progressive dehydration of antigorite. When the pore pressure becomes too high, a major fracturing event may occur (Dobson *et al.*, 2002). This tentatively explains the coexistence of ductile and brittle deformation at various scales, and is consistent with results of several experimental studies and seismological evidence. Indeed, embrittlement accounts for deep earthquakes within the subducting lithosphere (Peacock, 2001; Kerrick & Connolly, 2001; Dobson *et al.*, 2002; Jung *et al.*, 2003). Moreover, pressure solution is the most effective mechanism to accommodate deformation, and it is compatible with a Newtonian rheology for serpentinites as proposed by Gerya & Stöckert (2002). Moreover, their recurrent association with eclogite-facies rocks in paleo-subduction zones (Alps, Himalaya and the Caribbean) is consistent with the possible role of antigorite serpentinites in the preservation and exhumation of HP-LT rocks (Blake *et al.*, 1995; Hermann *et al.*, 2000; Schwartz *et al.*, 2000; Guillot *et al.*, 2000, 2001; Gerya & Stöckert, 2002). Indeed, serpentinites can localize the deformation within a subduction/exhumation channel, thus making it possible to preserve the structures and mineralogy of eclogites coming from depths > 100 km below the Earth's surface.

Acknowledgments: The authors are grateful to Prof. M. Mellini and Prof. F.J. Wicks for their helpful comments which led to significant improvements in the manuscript. This work benefited from fruitful discussions with I. Daniel, T.V. Gerya, K. Hattori, B. Stöcker and S. Schwartz. We also thank the CNRS/INSU DyETI programme for financial support and the CRMCN national facility for TEM.

References

Auzende, A-L., Devouard, B., Guillot, S., Daniel, I., Baronnet, A., Lardeaux, J-M. (2002): Serpentinites from Central Cuba: Petrology and HRTEM study. *Eur. J. Mineral.*, **14**, 905–914.

Bell, T.H. & Cluff, C. (1989): Dissolution, solution transfer, diffusion versus fluid flow and volume loss during deformation / metamorphism. *J. metamorphic Geol.*, **7**, 425–447.

Berman, R.G. (1988): Internally consistent thermodynamic data for minerals in the system Na_2O-K_2O-CaO-MgO-FeO-Fe_2O_3-SiO_2-TiO_2-H_2O-CO_2. *J. Petrol.*, **29**, 445–523.

Beyssac, O., Goffé, B., Chopin, C., Rouzaud, J.N. (2002): Raman spectra of carbonaceous material in metasediments: a new geothermometer. *J. metamorphic Geol.*, **20**, 859–871.

Blake, M.C., Moore, D.E., Jayko, A.S. (1995): The role of the serpentinite melange in the unroofing of UHPM rocks: an example from western Alps of Italy. *in* „Ultra high pressure metamorphism", Coleman, R.G., Wang, X. (Eds.), Cambridge University Press, 182–205.

Blenkisop, T. ((2000): Deformation microstructures and mechanisms in minerals and rocks. Kluwer Academic Publishers, Dordrecht/Boston/London, 150 pp.

Bons, A.J. & Schryvers, D. (1988): High resolution EM of stacking irregularities in chlorite crystals. *Ultramicroscopy*, **24**, 426.

Capitani, G. & Mellini, M. (2004): The modulated crystal structure of the „*odd*", *m* = 17, antigorite polysome. *Am. Mineral.*, **89**, 147–158.

Chapman, J.A. & Zussman, J. (1959): Further electron optical observations on crystal of antigorite. *Acta Cryst.*, **12**, 550–552.

Chiesa, S., Scambelluri, M. Forcella, F., Galli, M., Messiga, B., Pasquaré, G., Pedemonte, G.M., Piccardo, G.B., Rossi, P.M. (1975): Assetto strutturale ed interpretazione geodinamica del gruppo di Voltri. *Boll. Soc. Geol. It.*, **94**, 551–581.

Christoffensen, R. & Kronenberg, A. (1993): Dislocation interaction in experimentally deformed biotite. *J. Struct. Geol.*, **15**, 1077–1095.

Dobson, D.P., Meredith, P.G., Boon, S.A. (2002): Simulation of subduction zone seismicity by dehydration of serpentinite. *Science*, **298**, 1407–1410.

Dodony, I., Posfai, M. Buseck, P.R. (2002): Revised structure models for antigorite: An HRTEM study. *Am. Mineral.*, **87**, 1443–1457.

Durney, D.W. (1972): Solution transfert, an important geological deformation mechanism. *Nature*, **235**, 315–317.

Escartin, J., Hirth, G., Evans, B. (1997): Effects of serpentinization on the lithospheric strength and the style of normal faulting at slow-spreading ridges, *Earth Planet. Sci. Lett.*, **151**, 181–189.

Etheridge, M.A., Hobbs, B.E., Paterson, M.S. (1973): Experimental deformation of single crystals of Biotite. *Contrib. Mineral. Petrol.*, **38**, 21–36.

Evans, B.W. (2004): The serpentinite multisystem revisited: Chrysotile is metastable. *Intern. Geol. Rev.*, **46**, 479–506.

Evans, B.W., Johannes, W., Otterdoom, H., Trommsdorff, V. (1976): Stability of chrysotile and antigorite in the serpentine multisystem. *Schweiz. Mineral. Petrogr. Mitt.*, **56**, 79–93.

Fyfe, W.F. & McBirney, A.R. (1975): Subduction of the structure of andesitic belts. *Am. J. Sci.*, **275A**, 285–297.

Gerya, T.V. & Stöckert, B. (2002): Exhumation rates of high pressure metamorphic minerals in subduction channels: the effect of rheology. *Geophys. Res. Lett.*, **29**, 102–1-102–4.

Gray, D.R. (1979): Microstructure and crenulation cleavage differentiation: Implications on solution deposition processes. *J. Struct. Geol.*, **1**, 73–80.

Grobety, B. (2003): Polytypes and high-order structures of antigorite: A TEM study. *Am. Mineral.*, **88**, 27–36.

Guillot, S., Hattori, K.H., de Sigoyer, J. (2000): Mantle wedge serpentinization and exhumation of eclogites: Insights from Eastern Ladakh, Northwest Himalaya. *Geology*, **28**, 199–202.

Guillot, S., Hattori, K.H., de Sigoyer, J., Nägler, T., Auzende, A.L. (2001): Evidence of hydration of the mantle wedge and its role in the exhumation of eclogites. *Earth Planet. Sci. Lett.*, **193**, 115–127.

Hattori, K. & Guillot, S. (2003): Volcanic fronts as a consequence of serpentinite dehydration in the mantle wedge. *Geology*, **31**, 525–528.

Hermann, J., Müntener, O., Scambelluri, M. (2000): The importance of serpentine mylonites for subduction and exhumation of oceanic crust. *Tectonophysics*, **327**, 225–238.

Hyndman, R.D & Peacok, S.M. (2003): Serpentinization of the forearc. *Earth Planet. Sci. Lett.*, **212**, 417–432.

Jullien, M. (1995): Polytypisme, ordre d'empilement et interstratification dans la cookeite et les phyllosilicates non micacés du métamorphisme. Influence de la pression. PhD Thesis, Univ. Rennes, France, 226.

Jullien, M., Baronnet, A., Goffe, B. (1996): Ordering of the stacking sequence in cookeite with increasing pressure: An HRTEM study. *Am. Mineral.*, **81**, 67–78.

Jung, H., Dobrzhinetskaya, L.F., Green, H.W. (2003): Dehydration embrittlement of serpentine and its implications for earthquakes at depth. *EUG-AGU-EGS Joint Assembly*, **5**, Nice, France.

Kerrich, R. (1977): An historical review and synthesis of research on pressure solution. *Zentralbl. Geol. Paleontol.*, **1977**, 1, 512–550.

Kerrick, D.M. & Connolly, J.A.D. (2001): Metamorphic devolatilisation of subducted oceanic metabasalts: Implications for seismicity, arc magmatism and volatile recycling. *Earth Planet. Sci. Lett.*, **189**, 19–29.

Kronenberg, A.K., Kirby, S.H., Pinkston, J. (1990): Basal slip and mechanical anisotropy of biotite. *J. Geophys. Res.*, **95**, B12, 19257–19278.

Kunze, G. (1956): Die gewellte Struktur des Antigorits, I. *Zeitschrift für Kristallographie*, **108**, 82–107.

– (1958): Die gewellte Struktur des Antigorits, II. *Zeitschrift für Kristallographie*, **110**, 282–320.

– (1961): Antigorit. Strukturtheoretische Grundlagen und ihre praktische Bedeutung für die weitere Serpent-Forschung. *Fortschr. Mineral.*, **39**, 206–324.

Lagabrielle, Y. (1987): Les ophiolites: Marqueurs de l'histoire tectonique des domaines océaniques. Ph.D thesis, Univ. Bretagne Occidentale, 350 pp.

Lagabrielle, Y. & Lemoine, M. (1997): Alpine, Corsican and Apennine ophiolites: the slow-spreading ridge model. *C. R. Acad. Sci. Paris*, t. 325 Sér. II (**12**), 909–920.

Mares, V.M. & Kronenberg, A.K. (1993): Experimental deformation of muscovite. *J. Struct. Geol.*, **15**, 1061–1075.

Mellini, M. & Zussman, (1986) Carlosturanite (not picrolite) from Taberg, Sweden. *Mineral. Mag.*, **50**, 675–679.

Mellini, M., Trommsdorff, V., Compagnoni, R. (1987): Antigorite polysomatism: behaviour during progressive metamorphism. *Contrib. Mineral. Petrol.*, **97**, 147–155.

Messiga, B. & Scambelluri, M. (1991): Retrograde PTt path for the Voltri Massif eclogites (Liguran Alps, Italy): Some tectonic implications. *J. Metamorphic Geol.*, **9**, 93–109.

Messiga, B., Kienast, J.R., Rebay, G., Riccardi, P., Tribuzio, R. (1999): Cr rich magnesiochloritoïd eclogites from the Monviso ophiolites (Western Alps, Italy). *J. Metamorphic Geol.*, **17**, 287–299.

Mevel, C. (2003): Serpentinization of abyssal peridotites at mid-ocean ridges. *C.R. Geosciences*, **335**, 825–852.

Neufeld, K., Stretton, I.C., Mackwell, S.J. (2003): Deformation and dehydration interactions in serpentinite under orogenic conditions. *EGS-AGU-EUG Joint Assembly*, **5**, EAE03-A-05661.

O'Hanley, D.S. (1996): Serpentinites: Record of tectonic and petrological history. *Oxford Monographs on geology and geophysics*, **34**, Oxford University Press.

Otten, M.T. (1993): High resolution electron microscopy of polysomatism and stacking defects in antigorite. *Am. Mineral.*, **78**, 75–84.

Peacock, S.M. (2001): Are double seismic zones caused by serpentine dehydration reactions in the subducting oceanic mantle? *Geology*, **29**, 299–302.

Phillipot, P. (1993): Fluid melt interaction in mafic eclogites and coesite-bearing metasediments: constraints on volatile recycling during subduction. *Chemical Geol.*, **108**, 93–112.

Piccardo, G.B. (1984): Le ofioliti metamorfiche del gruppo di Voltri, Alpi Liguri: caratteri primari ed interpretazione geodinamica. *Mem. Soc. Geol. It*., **28**, 95–114.

Piccardo, G.B., Rampone, E., Scambelluri, M. (1988): The alpine evolution of the Erro-Tobbio peridotites (Voltri Massif – Ligurian Alps): some field and petrographic constraints. *Ofioliti*, **13**, 169–174.

Polino, R., Dal Piaz, G.V., Gosso, G. (1990): Tectonic erosion at the Adria margin and accretionnary processes for the cretaceous orogeny of the Alps. *Mém. Soc. Géol. France*, **156**, 345–367.

Raleigh, C.B. & Paterson, M.S. (1965): Experimental deformation of serpentinite and its tectonic implications. *J. Geophys. Res*., **70**, 3965–3985.

Scambelluri, M., Müntener, O., Hermann, J., Piccardo, G.B., Trommsdorff, V. (1995): Subduction of water in the mantle: History of an Alpine peridotite. *Geology*, **23**, 459–462.

Scambelluri, M., Bottazzi, P., Trommsdorff, V., Vannucci, R., Hermann, J., Gomez-Pugnaire, M.T., Vizcaino, V. (2001): Incompatible element-rich fluids released in deeply subducted mantle. *Earth Planet. Sci. Lett.*, **192**, 457–470.

Schwartz, S., Lardeaux, J.M., Guillot, S., Tricart, P. (2000): Diversité du métamorphisme éclogitique dans le massif ophiolitique du Monviso (Alpes occidentales, Italie). *Geodyn. Acta*, **13**, 169–188.

Schwartz, S., Allemand, P., Guillot, S. (2001): Numerical model of effect of serpentinites on the exhumation of eclogitic rocks: insights from the Monviso ophiolitic massif (Western Alps). *Tectonophysics*, **342**, 193–206.

Spinnler, G.E. (1985): HRTEM study of antigorite, pyroxene, serpentine reactions and chlorite. Ph.D thesis, Arizona State Univ., Tempe, Arizona.

Uehara, S. (1998): TEM and XRD studies of antigorite superstructure. *Can. Mineral.*, **36**, 1595–1605.

Uehara, S. & Shirozu, H. (1985): Variations in chemical composition and structural properties of antigorite. *Mineral. Mag.*, **12**, 299–318.

Ulmer, P. & Trommsdorff, V. (1995): Serpentine stability to mantle depths and subduction-related magmatism. *Science*, **268**, 858–861.

Viti, C. & Mellini, M. (1996): Vein antigorites from Elba Island, Italy. *Eur. J. Mineral.*, **8**, 423–434.

Wicks, F.J. & O'Hanley, D. (1988): Serpentine Minerals: Structure and petrology. *in* "Reviews in Mineralogy. Hydrous Phyllosilicates", Ed. Bailey, S.W., **19**, 91–167.

Wood, D.S. (1974): Current views of the development of slaty cleavage. *Ann. Rev. Earth Sci.*, **2**, 1–35.

Wunder, B. & Schreyer, W. (1997): Antigorite: High-pressure stability in the system MgO-SiO_2-H_2O (MSH). *Lithos*, **41**, 213–227.

Wunder, B., Wirth, R., Gottschalk, M. (2001): Antigorite: Pressure and temperature dependence of polysomatism and water content. *Eur. J. Mineral.*, **13**, 485–495.

Yada, K. (1979): Microstructures of chrysotile and antigorite by high-resolution electron microscopy. *Can. Mineral.*, **17**, 679–691.

Zussman, J. (1954): Investigation of the crystal structure of antigorite. *Mineral Mag.*, **30**, 498–512.

Zussman, J., Brindley, G.W., Comer, J.J. (1957): Electron diffraction studies of serpentine minerals. *Am. Mineral.*, **42**, 666–670.

Received 12 November 2004
Modified version received 21 June 2005
Accepted 19 September 2005